frontiers in Materials

ORIGINAL RESEARCH
published: 03 December 2019
doi: 10.3389/fmats.2019.00316

Magnetic Iron Sulfide Nanoparticles as Thrombolytic Agents for Magnetocaloric Therapy and Photothermal Therapy of Thrombosis

Dapeng Fu[1,2†], *Junle Liu*[2†], *Qilong Ren*[3], *Jinhui Ding*[2*], *Heyi Ding*[2], *Xuan Chen*[2] and *Xiaohu Ge*[1,4*]

[1] Xinjiang Medical University, Urumqi, China, [2] Department of Vascular Surgery, Karamay Central Hospital, Karamay, China, [3] Material Science and Engineering School, Donghua University, Shanghai, China, [4] Department of Vascular Surgery, The People's Hospital of Xinjiang Uygur Autonomous Region, Urumqi, China

OPEN ACCESS

Edited by:
Ming Ma,
Shanghai Institute of Ceramics (CAS), China

Reviewed by:
Xijian Liu,
Shanghai University of Engineering Sciences, China
Jinbao Qin,
Shanghai Ninth People's Hospital, China

***Correspondence:**
Jinhui Ding
2817602110@qq.com
Xiaohu Ge
549468587@qq.com

[†]These authors have contributed equally to this work

Specialty section:
This article was submitted to Biomaterials, a section of the journal Frontiers in Materials

Received: 15 October 2019
Accepted: 20 November 2019
Published: 03 December 2019

Citation:
Fu D, Liu J, Ren Q, Ding J, Ding H, Chen X and Ge X (2019) Magnetic Iron Sulfide Nanoparticles as Thrombolytic Agents for Magnetocaloric Therapy and Photothermal Therapy of Thrombosis. Front. Mater. 6:316. doi: 10.3389/fmats.2019.00316

Non-invasive removal of thrombosis is a difficult problem in clinical vascular disease. Herein, we reported magnetic hyperthermia combined photothermal therapy for celiac vein thrombosis using Fe_3S_4 nanoparticles as thrombolytic agents under the stimulation of a near infrared (NIR) laser and an external alternating magnetic field (AMF). Fe_3S_4 nanoparticles showed excellent magnetothermal conversion performance under the continuous stimulation of an AMF and very good photothermal conversion performance under the irradiation of a NIR laser. Moreover, Fe_3S_4 nanoparticles exhibited a synergistic thermal conversion effect under the co-stimulation of NIR and AMF. In addition, the Fe_3S_4 nanoparticles possess the ability for magnetic resonance (MR) imaging with the transverse relaxivity (r_2) is up to 53.1 mM^{-1} s^{-1}. Finally, we, for the first time, proved the Fe_3S_4 nanoparticles as a promising thrombolytic agent for both photothermal thrombolytic capacity and magnetothermal thrombolytic ability. Our work provides the insight of hyperthermia for removal of the thrombosis.

Keywords: photothermal therapy, magnetocaloric therapy, thrombosis, iron sulfide, magnetic resonance imaging

INTRODUCTION

Cardiovascular disease is one of the main causes of harm to human health (Mackman, 2008; Engelmann and Massberg, 2013). Because the blood vessels are aging and the blood vessel wall is damaged, it is easy to form the thromboses in the blood vessel, and it is also more likely to suffer from diseases such as hypertension and arteriosclerosis. Surgery and chemotherapy are still the main treatment options for thrombosis. Surgical treatment causes great pain to the patient's body; chemotherapy is non-targeting and belongs to systemic administration, which has great side effects (Voros et al., 2015). Traditional treatments often treat known thrombi, but may cause new problems for blood vessels. Older people with thrombosis often do not dare to use thrombolytic drugs. Therefore, it is of great significance to develop an efficient and accurate thrombosis treatment system for non-invasive and precise treatment of thrombosis.

Clinically approved thrombolytic agents are characterized by short half-life, short blood flow life and damage to local bleeding (Hacke et al., 2008; Derex and Nighoghossian, 2009). Nanoparticles have proven to be promising diagnostic agents for the treatment of a

variety of diseases and have relatively long blood circulation agents (Vogel and Venugopalan, 2003; Mahmoudi et al., 2011; Li et al., 2017). At present, it has been reported that hyperthermia can achieve a good thrombolytic effect (Voros et al., 2015; Wang X. et al., 2017). Hyperthermia methods include photothermal therapy and magnetic hyperthermia (Dai et al., 2019). Photothermal therapy is the treatment through heat generated by near-infrared (NIR) light-induced photothermal reagents (Fang et al., 2012; Zhang et al., 2013; Chen et al., 2014; Li et al., 2014, 2015, 2017). Wang et al. prove that heat generated by the photothermal effect of gold can achieve the purpose of thrombolysis (Wang X. et al., 2017). Magnetic hyperthermia is a way in which a magnetothermal conversion reagent generates heat to treat a disease under the action of an external alternating magnetic field (AMF) (Wang F. et al., 2017; Li et al., 2018; Dai et al., 2019). The magnetocaloric effect of iron oxide has been shown to accelerate the dissolution of blood clots in Voros et al.' report (Voros et al., 2015). However, there are more or less defects in the way of thrombolysis. In the photothermal treatment, due to the poor penetration of light, it is impossible to treat deep thrombus, such as celiac vein thrombosis. In the case of iron oxide magnetothermal treatment of thrombus, it causes certain side effects due to the long-term presence of iron oxide in the body. Therefore, there is a great of necessary and importance to adjust the current strategy for treating thrombosis to treat thrombosis.

Fe_3S_4 nanoparticles have similar properties to iron oxide (Liu et al., 2014). It has been revealed that Fe_3S_4 nanoparticles have a very good magnetocaloric effect which could be used in magnetic hyperthermia for deep thrombosis (Guan et al., 2018; Moore et al., 2019). Moreover, Fe_3S_4 nanoparticles have been shown to degrade rapidly *in vivo* (Guan et al., 2018). Therefore, Fe_3S_4 nanoparticles show great potential for the magnetic hyperthermia for deep thrombosis. Herein, we reported hyperthermia for celiac vein thrombosis using Fe_3S_4 nanoparticles as a thrombolytic reagent under the stimulation of a NIR laser and an AMF. Fe_3S_4 nanoparticles show a synergistic thermal transition effect under the co-action of a NIR laser and an AMF. In addition, the Fe_3S_4 nanoparticles possess the ability for magnetic resonance (MR) imaging with the transverse relaxivity (r_2) is up to 53.1 mM^{-1} s^{-1}. Finally, we, for the first time, proved the Fe_3S_4 nanoparticles as a promising thrombolytic agent for magnetic hyperthermia for celiac vein thrombosis.

RESULTS AND DISCUSSION

Synthesis and Characterization of Fe_3S_4 Nanoparticles

Hydrophilic Fe_3S_4 nanoparticles were synthesized via a simple hydrothermal method by reaction the $FeSO_4$ with L-Cysteine in water at 220°C for 20 h. During the preparation, the polyvinylpyrrolidone (PVP) was added into the reaction as surface ligand to improve their biocompatibility. Thus, the Fe_3S_4 nanoparticles are capped by PVP (demonstrated by FTIR, **Figure S1**) and hydrophilic, and can be used as thrombolytic agents without any further modification. As shown in **Figure 1A**, transmission electron microscopy (TEM) image demonstrated that the as-prepared products were highly dispersible nanoparticles. The size of NCs was found to be 17.7 nm based on the TEM images (**Figure S2**). More microstructure information can be achieved from high resolution TEM (**Figure 1B**). It shows an interplanar spacing of 0.298 nm, which can be indexed to (220) planes of greigite structured Fe_3S_4. As shown in **Figure 1C**, X-ray diffraction (XRD) pattern of the products could be well-matched with that of greigite structured Fe_3S_4 (JCPDS file no.: 16-0713), indicating that we obtained pure greigite structured Fe_3S_4 with high crystallinity. X-ray photoelectron spectroscopy (XPS) revealed the composition and element state of the as-prepared products (**Figure S3**). It showed that the products mainly contain Fe and S elements with no other impurities. We analyzed the valency state of Fe in Fe_3S_4 nanoparticles. **Figure 1D** shows Fe 2p spectrum for the Fe_3S_4 nanoparticles. It was demonstrated that there was a mixed Fe oxidation state, i.e., Fe^{2+} and Fe^{3+} (Guan et al., 2018), indicating a defect structure in Fe_3S_4 nanoparticles. According to the above results, it can be concluded that the pure Fe_3S_4 nanoparticles with high crystallinity was successfully formed.

Magnetocaloric Conversion Performance of Fe_3S_4 Nanoparticles

Figures 2A,B shows the magnetocaloric conversion performance of Fe_3S_4 nanoparticles. Under the continuous simulation of AMF (4.2×10^9 A m^{-1} s^{-1}), the temperature of Fe_3S_4 nanoparticles with a concentration of 0.5 mg/mL can increase by 12.8°C, while the temperature change of pure water is not obvious. When the concentration is increased to 1.0 mg/mL, the temperature of Fe_3S_4 nanoparticle dispersion can be raised by 20°C which is high enough to dissolve thrombus. **Figure 2C** shows the thermal imaging of pure water and Fe_3S_4 nanoparticles (1.0 mg/mL) under the action of an AMF for 5 min, respectively. As we can see from **Figure 2D**, a high contrast image was obtained. These results indicated that Fe_3S_4 nanoparticles showed an excellent magnetocaloric conversion performance.

Photothermal Conversion Performance of Fe_3S_4 Nanoparticles

We also measured the UV-vis absorbance spectrum of the Fe_3S_4 nanoparticles, which is important for photothermal performance. From **Figure 3A**, we can see that the Fe_3S_4 nanoparticles showed a strong absorption in the NIR region from 700 to 1,000 nm, resulted from the defect structure in Fe_3S_4 nanoparticles. Then varied concentrations (0–0.5 mg/mL) of Fe_3S_4 nanoparticles were exposed to an 808 nm (0.33 W cm^{-2}) laser to evaluate the photothermal effect. As expected, the Fe_3S_4 nanoparticles showed a good photothermal conversion performance with concentration-dependent photothermal effect (**Figure 3B**). Fe_3S_4 nanoparticles with a concentration at 0.5 mg/mL, the temperature can increase by about 30°C, while the temperature of pure water showed little change. The photothermal performance of Fe_3S_4 nanoparticles ensured the potential of Fe_3S_4 nanoparticles as a thrombolytic reagent.

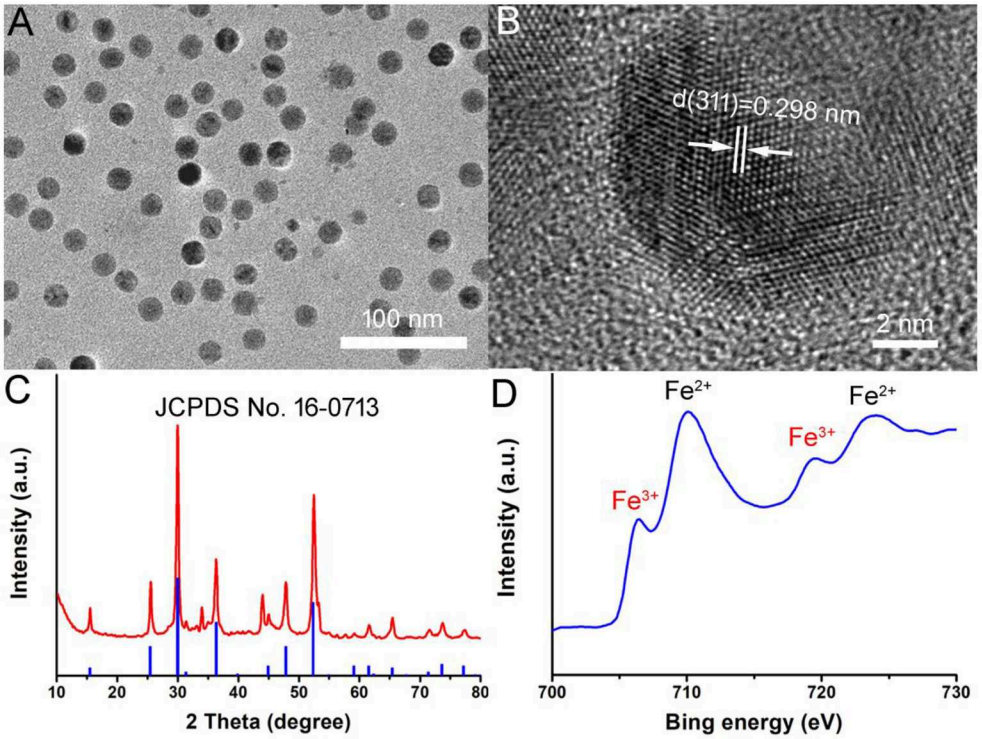

FIGURE 1 | (A) TEM image of as-prepared Fe_3S_4 nanoparticles. **(B)** High resolution TEM image of Fe_3S_4 nanoparticles. **(C)** XRD pattern of Fe_3S_4 nanoparticles. **(D)** High resolution XPS spectra of Fe in Fe_3S_4 nanoparticles.

Synergistic Thermal Conversion Effect

To test the synergistic thermal conversion effect of Fe_3S_4 nanoparticles, Fe_3S_4 nanoparticles (500 ppm, 100 μL) was assessed under the simultaneous stimulation including a NIR (808 nm, 0.33 W cm^{-2}) laser and an AMF (4.2×10^9 A m^{-1} s^{-1}) for 5 min. Temperature change was recorded by a thermal imaging camera. It was found that the temperature elevation can reach 37.1°C under the co-stimulation of NIR and AMF (**Figure 4A**). From **Figure 4B**, we can see that the temperature change from the co-stimulation of NIR and AMF was much higher the that from the single stimulation of NIR or AMF, indicating a synergistic thermal conversion effect.

Combined Therapy of Thrombotic *in vitro*

Due to the excellent thermal conversion performance of Fe_3S_4 nanoparticles, we measured the *in vitro* thrombolytic capacity of Fe_3S_4 nanoparticles under an 808 nm (0.33 W cm^{-2}) laser and/or an AMF (4.2×10^9 A m^{-1} s^{-1}). Thrombosis was obtained 1 week after ligation of the abdominal vena cava in mice using the surgical suture. A thrombus block was placed in a 20 mL glass vial followed by a 5 mL Fe_3S_4 nanoparticle solution. Finally, it was irradiated by an 808 nm (0.33 W cm^{-2}) laser and/or an AMF (4.2×10^9 A m^{-1} s^{-1}) for *in vitro* thrombolysis. As a control, the thrombus block in another bottle containing nanoparticle solution wasn't stimulated by NIR laser. It showed that the thrombus can be partially dissolved under the stimulation of NIR or AMF combined with Fe_3S_4 nanoparticles. Moreover, when co-stimulated by NIR and AMF, the thrombus was almost disappeared (**Figure S4**). However, the thrombus in the control showed little change. Therefore, Fe_3S_4 nanoparticles can be used as a thrombolytic agent under the stimulation of NIR or/and AMF.

MR Imaging Guided Thrombotic *in vivo*

Fe_3S_4 nanoparticles can be served for imaging guided magnetic hyperthermia of thrombosis. We established a model of deep vein thrombosis using black C57 mice, and the penetration depth of the laser did not reach the lesions. Moreover, the temperature of the hair of the C57 mice increased after laser irradiation to cause burntness. So we use magnetic hyperthermia to dissolve the thrombus. First, Fe_3S_4 nanoparticle' phantom images and proton T_2 relaxation test at varied Fe concentrations were measured. As shown in **Figure 5A**, T_2-weighted MR imaging signal intensity was increased with the increase of the concentration of Fe_3S_4 nanoparticle. The transverse relaxivity (r_2) value of the CMO NCs was calculated to be 53.1 mM^{-1} s^{-1}, indicating an efficient MRI contrast agent (**Figure 5B**). We then evaluated animal experiments on the T_2-weighted MR imaging guided magnetic hyperthermia of thrombosis. From **Figure 5C**, we can see that the signal in thrombosis sites (left) was light white. Under the action of Fe_3S_4 nanoparticles combined with AMF, light white region in thrombosis sites (right) obviously decreased. Therefore, Fe_3S_4

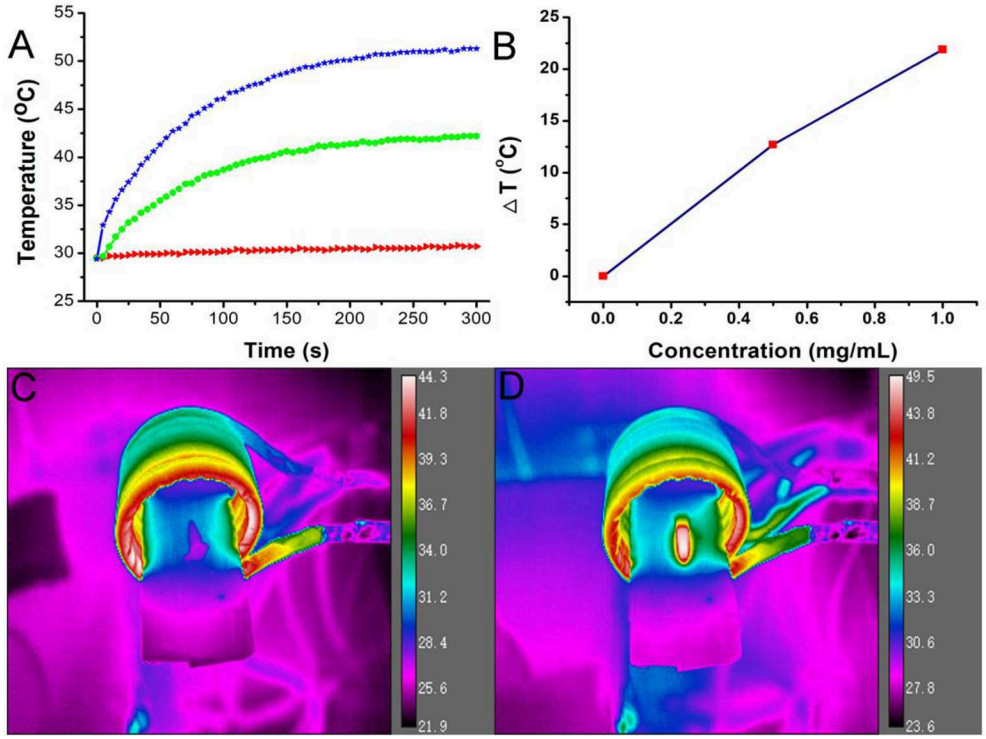

FIGURE 2 | (A) Temperature change of the Fe_3S_4 nanoparticles in water at varied concentrations of Fe^{2+} (i.e., 0, 0.5, and 1.0 mg/mL) as a function of magnetic field action time. **(B)** Plot of temperature change over 300s vs. the concentration of Fe_3S_4 nanoparticles. Thermal imaging of **(C)** pure water and **(D)** Fe_3S_4 nanoparticles (1.0 mg/mL) under the action of an AMF for 5 min.

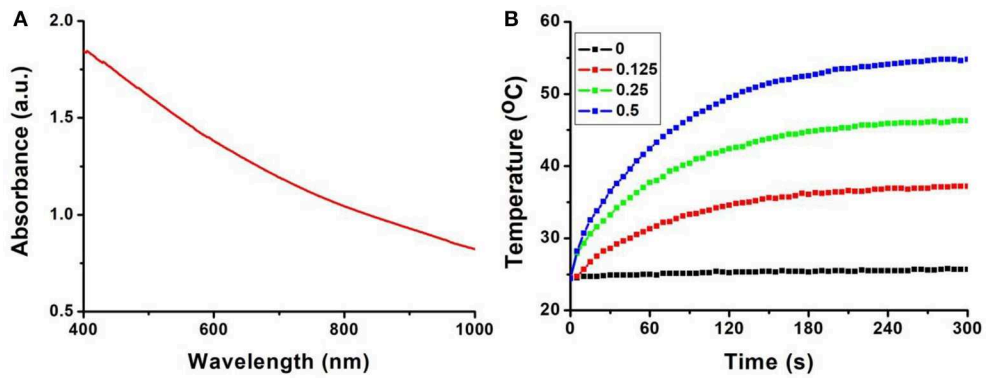

FIGURE 3 | (A) UV-vis absorbance spectrum of the Fe_3S_4 nanoparticles. **(B)** Temperature change of the Fe_3S_4 nanoparticles in water at varied concentrations (i.e., 0, 0.125, 0.25, and 0.5 mg/mL) as a function of the irradiation time of an 808 nm laser (0.33 W cm^{-2}).

nanoparticles can be served as an efficient thrombolytic agent *in vivo*.

Biomaterials must have good biocompatibility in clinical applications. Then *in vivo* long-term toxicity of the as-prepared Fe_3S_4 nanoparticles was evaluated by blood bioanalysis and hematoxylin and Eosin analysis, respectively. There was no obvious difference detected in alanine aminotransferase (ALT) and aspartate aminotransferase (AST) (**Figures 6A,B**), which indicated that Fe_3S_4 nanoparticles have good biocompatibility to the liver and heart (Zhang et al., 2018). Then histological examination analysis for main organs was performed to observe the shape and the size of cells after the intravenous injection of Fe_3S_4 nanoparticles at a dosage of 12 mg/kg. The organs included the heart, kidney, liver, lung, and spleen. As shown in **Figure 6C**, there is no tissue damage or adverse effect compared with those of control groups. This suggests

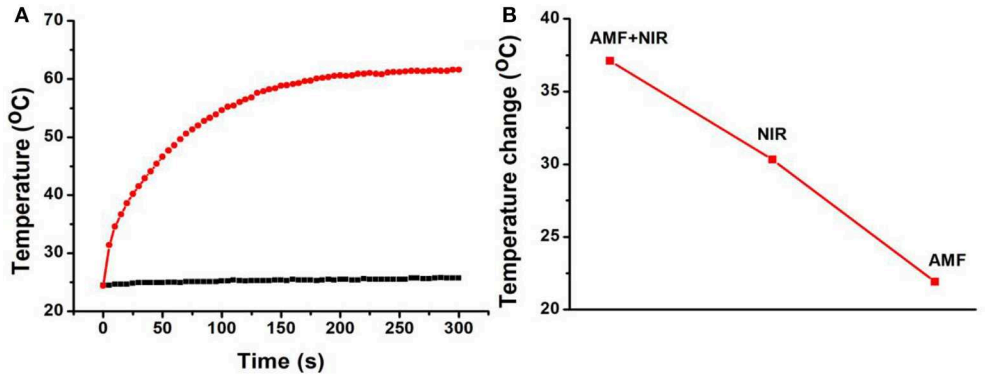

FIGURE 4 | (A) Temperature change of Fe_3S_4 nanoparticles under co-stimulation of NIR and AMF for 5 min. **(B)** Comparison of the temperature change from the indicated conditions. Fe_3S_4 nanoparticles: 0.5 mg/mL; NIR: 808 nm, 0.33 W cm^{-2}; AMF: 4.2 × 10^9 A m^{-1} s^{-1}.

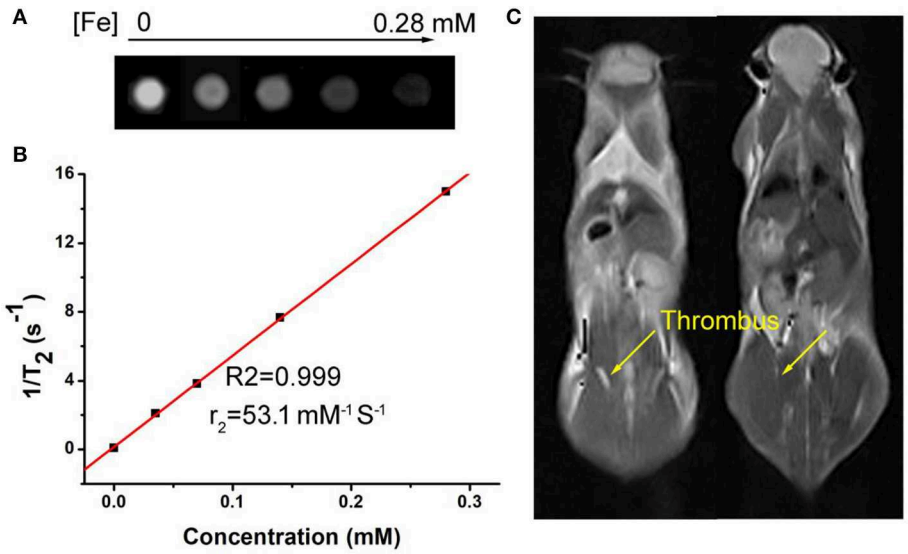

FIGURE 5 | (A) Phantom images of the Fe_3S_4 nanoparticles. **(B)** Proton T_2 relaxation measurements at varied Fe concentrations **(C)** T_2-weighted MR imaging *in vivo* of a mouse with celiac vein thrombosis before (left) and after (right) an intravenous injection of a solution of the Fe_3S_4 nanoparticles followed by the simulation of AMF.

that these Fe_3S_4 nanoparticles at the given dose are not obviously toxic.

It was reported that inorganic nanoparticles (quantum dots used as a model system) with relatively large sizes would accumulate in reticuloendothelial systems (RES) such as liver and spleen for long periods of time (Choi et al., 2007). Ideally, it would be the best to make Fe_3S_4 nanoparticles quickly excreted from the normal organs of the body, while being able to effectively accumulate and retain in lesions. A study from guan reported that the clearance of Fe_3S_4 nanoparticles was quickly post intravenous injection (Guan et al., 2018). We also studied the distribution and metabolism of the Fe_3S_4 nanoparticles, mice were intravenously injected with 12 mg·kg^{-1} of the Fe_3S_4 nanoparticles. At different intervals of time (i.e., 1, 3, 7, and 10 days, $n = 3$ at each time point), mice were sacrificed to obtain major organs including kidney, spleen, heart, liver, and lung. These organs were digested and solubilized. An ICP-MS analysis was used to determine Fe content in each organ. It was (**Figure S5**) found that the Fe_3S_4 nanoparticles mainly accumulate at spleen and liver, indicating that Fe_3S_4 nanoparticles was mainly degraded in these two organs.

CONCLUSION

In conclusion, Fe_3S_4 nanoparticles, as a new imaging-guided thrombolytic agent, have been successfully prepared by a simple hydrothermal route. The as-prepared Fe_3S_4 nanoparticles have a good dispersity and show an excellent magnetothermal conversion performance and photothermal effect, and exhibited a synergistic thermal conversion effect under the co-stimulation of NIR and AMF. They also possess an effective MR imaging *in vivo*. Furthermore, the *in vivo* toxicity results indicate their excellent biocompatibility. With the stimulation of an external AMF and

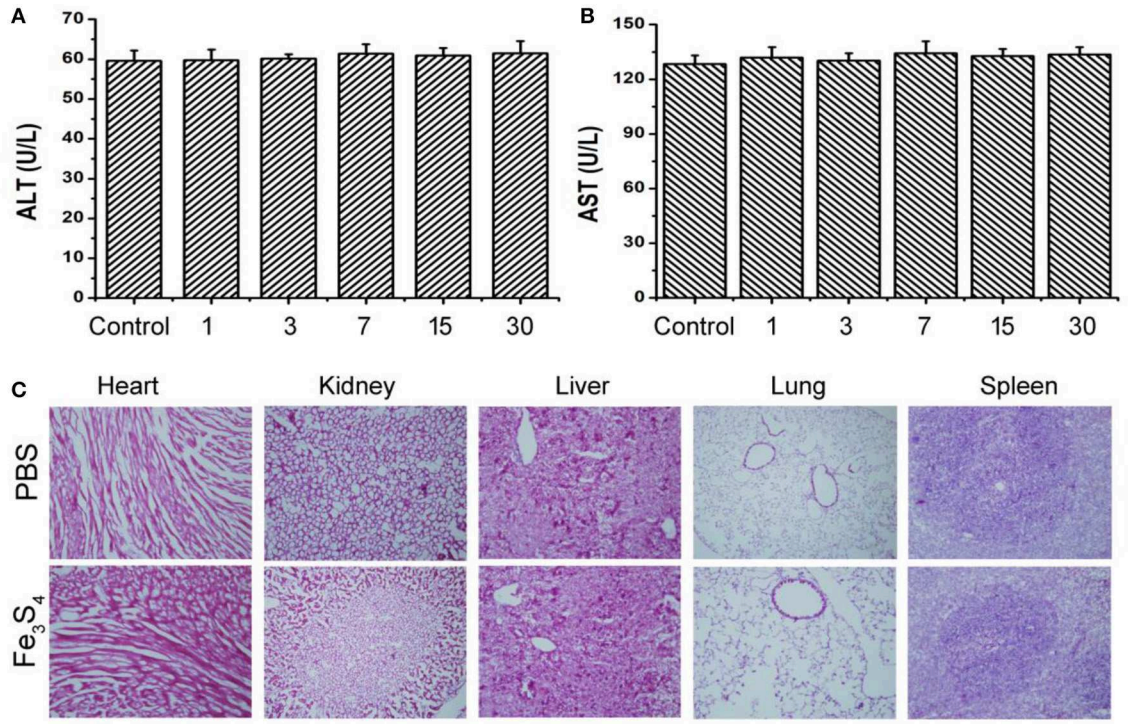

FIGURE 6 | Blood bioanalysis of mice in control group and Fe_3S_4 group at different time points (1, 3, 7, 15, and 30 days), including **(A)** alanine aminotransferase (ALT) and **(B)** aspartate aminotransferase (AST). **(C)** Hematoxylin and Eosin stained tissue sections from the mice to monitor the histological changes in heart, kidney, liver, lung, and spleen of the mice 1 month after a single intravenous injection of the Fe_3S_4 nanoparticle' solution. Scale bar: 100 μm.

a NIR laser, the Fe_3S_4 nanoparticles can be used as thrombolytic agents with MR imaging guided hyperthermia of thrombosis.

EXPERIMENTAL SECTIONS

Synthesis of Fe_3S_4 Nanoparticles

One millimole of $FeSO_4$ and 1 mmol L-cysteine were consecutively dissolved in 40 mL water. Seven hundred milligram of poly (vinyl pyrrolidone) (PVP) was then added. Then the reaction was kept at 220°C for 24 h in a stainless steel autoclave. The products were collected through centrifugation and finally washed with ethanol and deionized water for three times.

Characterization

The morphology as well as the size of nanoparticles was achieved by TEM (JEOL JEM-2010F, Japan). The crystal phase of Fe_3S_4 nanoparticles was measured by XRD (Bruker D4). The oxidation state analysis of Fe_3S_4 nanoparticles was measured by X-ray photoelectron spectra (XPS, ESCA-Lab 250Xi). Concentration of Fe ions released from Fe_3S_4 nanoparticles was tested by ICP-AES (Leeman Laboratories Prodigy).

Measurement of Magnetocaloric Conversion Performance of Fe_3S_4 Nanoparticles

For the evaluation of the magnetocaloric conversion performance of Fe_3S_4 nanoparticles, 100 μL of Fe_3S_4 nanoparticles dispersed in deionized water at varied concentrations was simulated under the external AMF (4.2 $\times$ 10^9 A m^{-1} s^{-1}). Temperature change was recorded by a thermal imaging camera.

Measurement of Photothermal Effect of Fe_3S_4 Nanoparticles

For the evaluation of the photothermal performance of Fe_3S_4 nanoparticles, 100 μL of Fe_3S_4 nanoparticles dispersed in deionized water at varied concentrations was exposed upon the irradiation of an 808 nm laser. Temperature change was recorded by a thermal imaging camera.

Thrombotic Animal Model

All animal experiments were approved by the Animal Ethics Committee of Karamay central hospital. 8-week-old C57 mice were anesthetized and laparotomy, the inferior vena cava was separated, and the inferior vena cava was ligated under the left renal vein with a surgical line (Kyogashima et al., 1999).

Hyperthermia of Thrombosis *in vitro*

To evaluate *in vitro* thrombolytic capacity of Fe_3S_4 nanoparticles under the irradiation of a NIR laser or/and AMF, thromboses was obtained 1 week after ligation of the abdominal vena cava in mice using a surgical line. A thrombus block was placed in a 20 mL glass vial followed by a 5 mL Fe_3S_4 nanoparticle solution. Finally, it was irradiated by an 808 nm laser or/and AMF for *in vitro* thrombolysis. As a control, the thrombus block in another

bottle containing nanoparticle solution wasn't stimulated by the 808 nm laser or/and AMF.

MR Imaging Guided Hyperthermia of Thrombosis *in vivo*

The Fe_3S_4 nanoparticle dispersions with varied Fe concentrations (0–0.28 mM) were scanned at room temperature via the animal MR imagine scanner under a 0.5 T MRI scanner at room temperature. Before *in vivo* MR imaging guided magnetic hyperthermia of thrombosis, thrombosis model mouse were scanned with the same MR scanner with the same parameters to be a control. After intravenous injection with the Fe_3S_4 nanoparticle dispersion (100 μL, 12 mg/kg) followed by stimulation under an AMF, the thrombosis model mouse were scanned again with the MR scanner.

Histological Examination Analysis and Blood Analysis

As for the histological examination, one mouse in each group was killed under anesthesia after the indicated treatment. Then the organs included the heart, kidney, liver, lung, and spleen were harvested, and then sectioned into 4 μm slices using a conventional microtome, finally stained with H&E. The slices were examined via a microscope. Also, the blood from mice in control group and Fe_3S_4 group was collected to test the biocompatibility of Fe_3S_4 nanoparticle to major organs.

DATA AVAILABILITY STATEMENT

All datasets generated for this study are included in the article/**Supplementary Material**.

ETHICS STATEMENT

The animal study was reviewed and approved by the Animal Ethics Committee of Karamay Central Hospital.

AUTHOR CONTRIBUTIONS

DF, JD, and XG designed the project. DF, QR, JL, and HD carried out the experiment and performed the experimental data analysis. DF and XC wrote the paper. All the authors contributed to discussion of the results.

FUNDING

This work was supported by Xinjiang Uygur Autonomous Region Natural Science Fund (2019D01A08).

SUPPLEMENTARY MATERIAL

The Supplementary Material for this article can be found online at: https://www.frontiersin.org/articles/10.3389/fmats.2019.00316/full#supplementary-material

REFERENCES

Chen, Q., Wang, C., Zhan, Z., He, W., Cheng, Z., Li, Y., et al. (2014). Near-infrared dye bound albumin with separated imaging and therapy wavelength channels for imaging-guided photothermal therapy. *Biomaterials* 35, 8206–8214. doi: 10.1016/j.biomaterials.2014.06.013

Choi, H. S., Liu, W., Misra, P., Tanaka, E., Zimmer, J. P., Itty Ipe, B., et al. (2007). Renal clearance of quantum dots. *Nat. Biotechnol.* 25, 1165–1170. doi: 10.1038/nbt1340

Dai, C., Wang, C., Hu, R., Lin, H., Liu, Z., Yu, L., et al. (2019). Photonic/magnetic hyperthermia-synergistic nanocatalytic cancer therapy enabled by zero-valence iron nanocatalysts. *Biomaterials*, 219:119374. doi: 10.1016/j.biomaterials.2019.119374

Derex, L., and Nighoghossian, N. (2009). Thrombolysis, stroke-unit admission and early rehabilitation in elderly patients. *Nat. Rev. Neurol.* 5, 506–511. doi: 10.1038/nrneurol.2009.127

Engelmann, B., and Massberg, S. (2013). Thrombosis as an intravascular effector of innate immunity. *Nat. Rev. Immunol.* 13, 34–45. doi: 10.1038/nri3345

Fang, W., Yang, J., Gong, J., and Zheng, N. (2012). Photo- and pH-triggered release of anticancer drugs from mesoporous silica-coated Pd@Ag nanoparticles. *Adv. Funct. Mater.* 22, 842–848. doi: 10.1002/adfm.201101960

Guan, G., Wang, X., Li, B., Zhang, W., Cui, Z., Lu, X., et al. (2018). "Transformed" Fe_3S_4 tetragonal nanosheets: a high-efficiency and body-clearable agent for magnetic resonance imaging guided photothermal and chemodynamic synergistic therapy. *Nanoscale* 10, 17902–17911. doi: 10.1039/C8NR06507A

Hacke, W., Kaste, M., Bluhmki, E., Brozman, M., Dávalos, A., Guidetti, D., et al. (2008). Thrombolysis with alteplase 3 to 4.5 hours after acute ischemic stroke. *N. Engl. J. Med.* 359, 1317–1329. doi: 10.1056/NEJMoa0804656

Kyogashima, M., Onaya, J., Miyauchi, S., Arai, M., Shibata, Y., Suda, A., et al. (1999). Antithrombotic activity of avian crown dermatan sulfate. *Thromb. Res.* 96, 459–465. doi: 10.1016/S0049-3848(99)00138-3

Li, B., Wang, Q., Zou, R., Liu, X., Xu, K., Li, W., et al. (2014). Cu7.2S4 nanocrystals: a novel photothermal agent with a 56.7% photothermal conversion efficiency for photothermal therapy of cancer cells. *Nanoscale* 6, 3274–3282. doi: 10.1039/c3nr06242b

Li, B., Ye, K., Zhang, Y., Qin, J., Zou, R., Xu, K., et al. (2015). Photothermal theragnosis synergistic therapy based on bimetal sulphide nanocrystals rather than nanocomposites. *Adv. Mater. Weinheim.* 27, 1339–1345. doi: 10.1002/adma.201404257

Li, B., Yuan, F., He, G., Han, X., Wang, X., Qin, J., et al. (2017). Ultrasmall $CuCo_2S_4$ nanocrystals: all-in-one theragnosis nanoplatform with magnetic resonance/near-infrared imaging for efficiently photothermal therapy of tumors. *Adv. Funct. Mater.* 27:1606218. doi: 10.1002/adfm.201606218

Li, M., Bu, W., Ren, J., Li, J., Deng, L., Gao, M., et al. (2018). Enhanced synergism of thermo-chemotherapy for liver cancer with magnetothermally responsive nanocarriers. *Theranostics* 8, 693–709. doi: 10.7150/thno.21297

Liu, X., Feng, C., Bi, N., Sun, Y., Fan, J., Lv, Y., et al. (2014). Synthesis and electromagnetic properties of Fe_3S_4 nanoparticles. *Ceramics Int.* 40, 9917–9922. doi: 10.1016/j.ceramint.2014.02.087

Mackman, N. (2008). Triggers, targets and treatments for thrombosis. *Nature* 451, 914–918. doi: 10.1038/nature06797

Mahmoudi, M., Sant, S., Wang, B., Laurent, S., and Sen, T. (2011). Superparamagnetic iron oxide nanoparticles (SPIONs): development, surface modification and applications in chemotherapy. *Adv. Drug Deliv. Rev.* 63, 24–46. doi: 10.1016/j.addr.2010.05.006

Moore, J., Nienhuis, E., Ahmadzadeh, M., and McCloy, J. (2019). Synthesis of greigite (Fe_3S_4) particles via a hydrothermal method. *AIP Adv.* 9:035012. doi: 10.1063/1.5079759

Vogel, A., and Venugopalan, V. (2003). Mechanisms of pulsed laser ablation of biological tissues. *Chem. Rev.* 103, 577–644. doi: 10.1021/cr010379n

Voros, E., Cho, M. J., Ramirez, M., Palange, A. L., De Rosa, E., Key, J., et al. (2015). TPA immobilization on iron oxide nanocubes and localized magnetic

hyperthermia accelerate blood clot lysis. *Adv. Funct. Mater.* 25, 1709–1718. doi: 10.1002/adfm.201404354

Wang, F., Yang, Y., Ling, Y., Liu, J., Cai, X., Zhou, X., et al. (2017). Injectable and thermally contractible hydroxypropyl methyl cellulose/Fe_3O_4 for magnetic hyperthermia ablation of tumors. *Biomaterials* 128, 84–93. doi: 10.1016/j.biomaterials.2017.03.004

Wang, X., Wei, C., Liu, M., Yang, T., Zhou, W., Liu, Y., et al. (2017). Near-infrared triggered release of uPA from nanospheres for localized hyperthermia-enhanced thrombolysis. *Adv. Funct. Mater.* 27:1701824. doi: 10.1002/adfm.201701824

Zhang, W., Deng, G., Li, B., Zhao, X., Ji, T., Song, G., et al. (2018). Degradable rhenium trioxide nanocubes with high localized surface plasmon resonance absorbance like gold for photothermal theranostics. *Biomaterials* 159, 68–81. doi: 10.1016/j.biomaterials.2017.12.021

Zhang, Z., Wang, J., and Chen, C. (2013). Near-infrared light-mediated nanoplatforms for cancer thermo-chemotherapy and optical imaging. *Adv. Mater. Weinheim.* 25, 3869–3880. doi: 10.1002/adma.201301890

Conflict of Interest: The authors declare that the research was conducted in the absence of any commercial or financial relationships that could be construed as a potential conflict of interest.